

A Comparative Study into Two Dual Fluorescent Mechanisms via Positional Isomers of *N*-hydroxyarene-1,8-naphthalimides

Sangita Paudel · Premchendar Nandhikonda · Michael D. Heagy

Received: 29 July 2008 / Accepted: 16 January 2009 / Published online: 4 February 2009
© Springer Science + Business Media, LLC 2009

Abstract Three isomers of hydroxy substituted *N*-aryl-1,8-naphthalimides based on *N*-aryl naphthalic anhydride fluorophore have been synthesized. The decrease in fluorescence intensity from ortho to para substitution of hydroxy group on *N*-aryl reveals that para substituted isomer undergoes ESEC (Excited State with Extended Conjugation) mechanism which is proved by low quantum yield and appearance of dual emission. The ortho isomer, however, has high quantum yield and no tautomer emission, indicating ESIPT (Excited State Intramolecular Proton Transfer) mechanism is not operating. Similarly, all these isomers show strong fluorescence quenching in presence of strong H-bonding solvents like DMSO and pyridine, but there was neither the shift of emission bands nor the appearance of new bands for proton transfer to these solvents. Thus, it also indicates the absence of excited state proton transfer mechanism. Both the ortho isomer, and to a greater degree the meta isomer, showed larger quenching constants (K_{app}) with pyridine than DMSO. This trend opposes the hydrogen-bond affinity for these solvents with phenol and points to a 2-point recognition interaction. In addition, a naphthalimide derivative using 2-aminoimidazole was prepared and examined for optimal positioning of a six-membered ring hydrogen bond pattern. No dual fluorescence was observed for this compound either.

Keywords *N*-arylnaphthalimide · Dual fluorescence · ESIPT · ESEC

Introduction

Recently, the advantages of dual fluorescent (DF) dyes have been highlighted by Demchenko with particular regard to their application in multifunctional sensor microarrays and other microscale sensor systems [1]. Some key features obtained from such photophysical properties arise in the ability for self-calibration of instrumental factors and more accurate cellular imaging where the variation of density/concentration of sensor molecules in the illuminated and observed volume is the limiting factor for quantitative assays. Perhaps the most well studied and established photoprocesses systems are based on dimethylaminobenzonitrile (DMABN) dyes which have been shown to display two-color emission via internal charge transfer properties. A number of reports have shown that depending on the degree of steric hindrance about the donor and acceptor groups, the dual fluorescence arises from either a twisted intramolecular charge transfer (TICT) [2] or a planarized intramolecular charge transfer (PICT) [3–6]. A number of applications have evolved from this two-color response, most notably in the area of fluorescent molecular probes for ions and molecules [7–13].

Some of the photophysical processes currently published that account for two-color emission from non-TICT/PICT systems also have potentially useful applications, particularly in the area of analytical response. For example, dyes that undergo excited state intramolecular proton transfer (ESIPT) possess especially useful photophysical properties [14, 15]. These compounds display two well-separated emission bands that in most cases are of equal intensity [14, 15]. The ESIPT (Excited State Intramolecular Proton Transfer)

Electronic supplementary material The online version of this article (doi:10.1007/s10895-009-0462-2) contains supplementary material, which is available to authorized users.

S. Paudel · P. Nandhikonda · M. D. Heagy (✉)
Department of Chemistry, New Mexico Institute
of Mining & Technology,
801 Leroy Avenue,
Socorro, NM 87801, USA
e-mail: mheagy@nmt.edu

process was first reported by Albert Weller using 2-hydroxybenzoyl compounds such as methyl salicylate [16]. The ESIPT process is one of the most effective principles used in the design of molecules giving dual emission due to the formation of two tautomeric forms in the excited state [3–6]. This process usually occurs in organic bifunctional molecules containing both hydrogen atom donor groups like hydroxyl or amino groups and hydrogen atom acceptor groups like carbonyl groups in close proximity where an intramolecular hydrogen bond formation is possible in the electronic ground state. The electronic charge redistribution within the molecule due to photoexcitation causes the ESIPT process [14, 15]. The rate of ESIPT is very fast due to the slight movement (about 1 Å) of the very light hydrogen atom in the excited state and is complete within the picosecond time regime at room temperature [18].

Kasha et al. have extensively studied this mechanism using 3-hydroxyflavones (3HF). Intramolecular proton transfer has been observed in these hydroxyflavones in highly purified and extremely dry solvent [17]. Formosinho has extensively reviewed intramolecular excited state proton transfer of aromatic systems in relation to the nature of the hydrogen bond ring [18]. Brown et al. have also reviewed systems that pertain to hydroxy aromatic compounds [19]. Similarly, Dogra et al. have done an extensive research on this field using different derivatives of benzimidazole (BI), benzoxazole (BO), and benzothiazole (BT) moieties [20]. As Dogra et al. reported in their earlier work, the dual emission in 2-(2'-aminophenyl)benzimidazoles via ESIPT mechanism occurs only in nonpolar solvent. Later, to study the strong intramolecular H-bonding effect, one of the amino hydrogen atoms on the amino group was replaced by an acetyl group (electron withdrawing group). For this compound both the normal and the tautomer emissions were observed in all the solvents used. The presence of an acetyl group caused an appreciable increase in the acidity of amino proton leading to an increase in the rate of proton transfer.

More recently, 2-aryl-3-hydroxyquinolones were reported as a new set of quinolone dyes that display dual emission via ESIPT mechanism [21]. These 2-aryl-3-hydroxyquinolones with different electron donating aryl substituents at position 2 displayed the dual emission in all the tested solvents. For *N*-methyl substituted compounds of this class, the intensity ratio of the two emission bands was reported to be sensitive to solvent polarity with a change from toluene to dimethylsulfoxide. Another system that has been shown to display two emission bands even in protic systems such as water has generated considerable interest as a potential platform for fluorescent probes and operates through an excited state with extended conjugation mechanism (ESEC) [22]. Such dual fluorescent compounds are known as *N*-aryl-naphthalimides (NI) specifically the 1,2-, 2,3-, and 1,8- naphthalimides. An

important distinction made between NI based dyes and DMABN based dyes is that the long wave (LW) emission is not dependent on solvent polarity. In sharp contrast to PICT/TICT dyes, the dipole moment of *N*-aryl-naphthalimides has been found to be relatively small [23]. These fluorescent systems are thought to possess two emissive states *S*1 and *S*2, which are responsible for short wave (SW) and long wave (LW) emission, respectively [24]. While emission from *S*2 states are quite rare, the two excited state levels (*S*1 and *S*2) have an energy gap sufficiently small for vibronic coupling [24]. The calculated electron distributions for the relevant molecular orbitals involving *S*1 and *S*2 are given in Fig. 1. Electron transfer from the HOMO to the LUMO occurs from the π^* orbitals of the carbonyl groups to the naphthalene moiety, in which the electrons of the aniline group do not participate. This excited state transition is expected to relax via radiative decay as SW emission. A comparison between the electron distributions in HOMO-1 and LUMO orbitals, however, indicates that electron density undergoes a longer distance shift from the aniline ring to naphthalene moiety. This *S*2 state reverses the direction of the dipole moment in relation to the ground state, thus giving rise to charge-transfer character (ICT) states responsible for solvent stabilized LW fluorescence.

The geometry of SW state is considered to be similar to that of ground state while the geometry of LW state

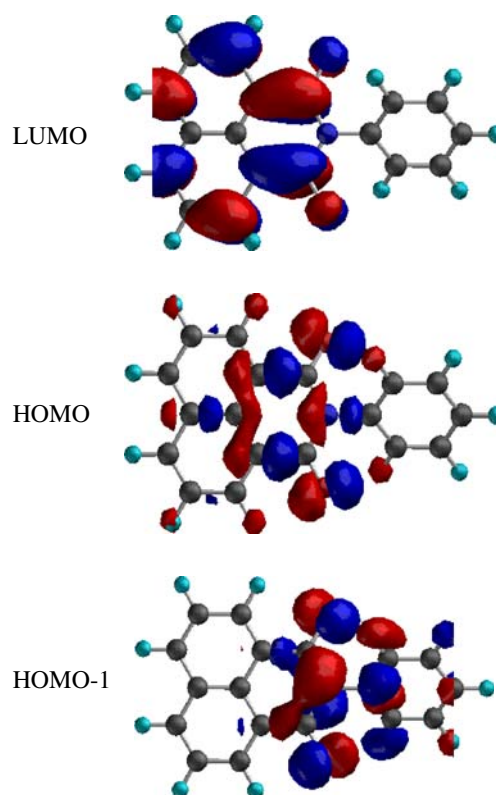


Fig. 1 Relevant molecular orbitals of *N*-phenyl-1,8-naphthalimide scaffold (adapted from ref 24)

assumes a coplanar conformation. The formation of SW state is assumed to be associated with charge transfer from the naphthalimide moiety to the π^* orbitals of the carbonyl group leading to an increase in the dipole moment of SW excited state in comparison to that of ground state. Similarly, the formation of LW state is the result of twisting of the phenyl group toward a coplanar geometry in which the driving force is the extra stability of the coplanar structure associated with the extended conjugation between the naphthalimide moiety and the phenyl group [20]. Substituent effects on both the naphthalimide moiety and the phenyl group have been studied to account for the trends in SW vs LW emission in *N*-aryl 1,8-naphthalimides [25]. According to this paper [25], the substituted naphthalimide moiety affects the SW excited state energy level while substituted *N*-aryl group affects the LW excited state energy level. Electron releasing substituents on both the naphthalimide moiety and the *N*-aryl group favor SW emission while no substituent on the naphthalimide moiety and the electron releasing group on *N*-aryl part favors LW emission or both SW and LW emissions (dual emission) [25].

This paper also reported the effect of the position of substituent on *N*-aryl part toward dual emission. Dual emission is only observed in *para* methoxy substituted *N*-aryl naphthalimides but not in *ortho* or *meta* substituted isomers of that compound. The absence of dual emission in either *ortho* or *meta* isomers of methoxy substituted *N*-aryl 1,8-naphthalimides is due to steric factors, and therefore, the prevention of phenyl rotation leading to a coplanar conformation. With the absence of extended conjugation between naphthalimide moiety and phenyl group, the ESEC mechanism is inoperative.

As part of our ongoing work involving *N*-aryl-1,8-naphthalimides, it occurred to us that certain hydroxyl substituted derivatives might operate under competing mechanism as either an ESIPT or ESEC depending on the geometrical constraints of the molecule. ESIPT has been shown to occur when a nearby Brønsted donor and acceptor are arranged within intramolecular five or six-member ring arrangement. Our aim in this comparative study involved the

preparation of *N*-aryl group substituted with a hydroxyl group specifically at the *ortho* position so that it may display photo physical features similar to an ESIPT dye or perhaps a combination of ESIPT and ESEC, and a *para* hydroxyl substituted isomer that may display dual emission via ESEC mechanism. In order to distinguish between two potentially competing mechanisms, the three positional isomers of aminophenol were incorporated into our synthesis of *N*-aryl-1,8-naphthalimides.

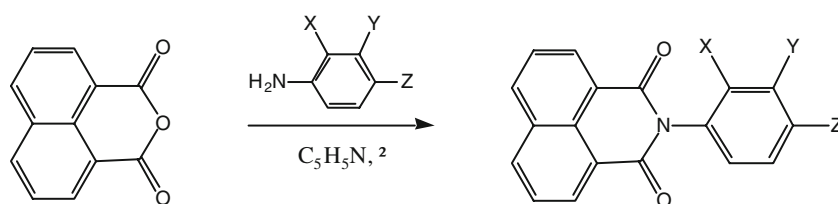
Similarly, the effect of position of hydroxyl groups on dual emission and on quantum yield will be investigated using these three isomers. Previous studies have also shown that the position of electron releasing groups on the *N*-aryl part of naphthalimides affects the dual emission character of such molecules. The synthesis of each of these three positional isomers was readily carried out with the three aminophenol isomers in condensation reaction (Scheme 1) with commercially available 1,8-naphthalimide anhydride. In addition, a fourth derivative of 1,8-naphthalimide with a more ideal six-membered hydrogen bond configuration was also prepared and included in this study. Specifically, 2-aminoimidazole was condensed with 1,8-naphthalic anhydride as shown in Scheme 2.

Experimental details

Methods

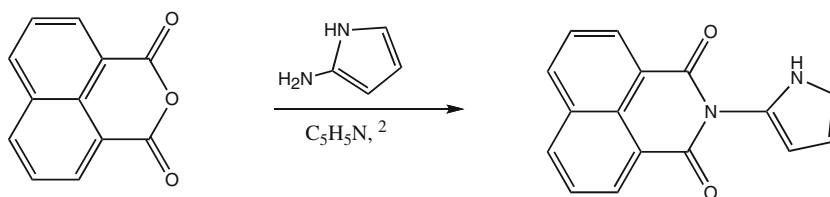
To synthesize these isomers, reactions were typically run overnight 16 h and thin layer chromatography revealed reaction products. The solvent pyridine was evaporated by passing compressed air over the solvent in a hood. For purification, a column was done using mixture of acetone and dichloromethane in different ratios for these different isomers. Finally, solvent was evaporated using rotary evaporator and a dry tan powder was obtained. IR spectra were recorded on a Nicolet Avatar 370 DTGS. ^1H NMR (300 MHz) and ^{13}C NMR (75 MHz) spectra were recorded on a JEOL Eclipse 300+ spectrometer. Merck precoated Silica gel 60 F₂₅₄ on prescored

Scheme 1 Synthesis of *N*-aryl-1,8-naphthalimides



1. X = OH, Y = H, Z = H
2. X = H, Y = OH, Z = H
3. X = H, Y = H, Z = OH

Scheme 2 Synthesis of N-imidazolyl-1,8-naphthalimides



glass were used for qualitative TLC. Spots were detected by UV-lamp. Elemental and analyses were performed by Galbraith Laboratories. Melting points were measured on a hot plate melting apparatus and were uncorrected.

Synthesis and characterization

N-(2'-hydroxyphenyl)-1,8-naphthalimide (1)

0.3 g (1.15 mmol) 1,8-naphthyl anhydride and 0.165 g (1.15 mmol) 3-amino phenol were taken in a 25 ml round bottom flask along with 4 ml pyridine and refluxed for overnight at about 140 °C. Pyridine was evaporated and crude product was purified with 1:1 dichloromethane and acetone in a short column packed with silica gel. After evaporating the solvent, 0.19 g (41%) of tan powder was obtained. m.p.: 228–230 °C, $^1\text{H NMR}$ (DMSO- d_6) δ : 8.5 (d, $J=8.0$ Hz, 4H), 7.8 (dd, $J=7.7$ Hz, 2H), 7.2 (dd, $J=8.3$ Hz, 1H), 6.7 (m, $J=8.5$ Hz, 3H), 9.6 (s, 1H); $^{13}\text{C NMR}$ (DMSO- d_6) δ : 164.1, 158.4, 137.4, 134.9, 131.9, 131.2, 130.0, 128.3, 127.7, 123.1, 120.1, 116.7, 115.7; IR $\nu=1701, 1649, 1585, 1357, 1298, 775, \text{cm}^{-1}$. Anal. Calcd. for $\text{C}_{18}\text{H}_{11}\text{NO}_3$: C, 74.7; H, 3.83; N, 4.84. Found: C, 74.43; H, 3.73.

N-(3'-hydroxyphenyl)-1,8-naphthalimide (2)

This compound was prepared in manner similar to the isomeric compound (1) starting with 0.3 g (1.15 mmol) 1,8-naphthyl anhydride and 0.165 g (1.15 mmol) 2-amino phenol. This reaction afforded 0.21 g (46%) tan powder as product. m.p.: 232–235 °C. $^1\text{H NMR}$ (DMSO- d_6) δ : 8.5 (d, $J=8.2$ Hz, 4H), 7.9 (dd, $J=7.7$ Hz, 2H), 7.2 (m, $J=7.7$ Hz, 2H), 6.9 (m, $J=7.9$ Hz, 2H), 9.6 (s, 1H); $^{13}\text{C NMR}$ (DMSO- d_6) δ : 163.9, 153.9, 134.9, 132, 131.1, 130.8, 130.1, 127.7, 123.5, 123.2, 119.6, 117.02; IR $\nu=1,703, 1,645, 1,587, 1,376, 1,238, 795 \text{ cm}^{-1}$. Anal. Calcd. for $\text{C}_{18}\text{H}_{11}\text{NO}_3$: C, 74.7; H, 3.83. Found: C, 74.43; H, 3.80.

N-(4'-hydroxyphenyl)-1,8-naphthalimide (3)

0.2 g (1.01 mmol) of 1,8-naphthalene dicarboxylic anhydride and 0.12 g (1.10 mmol) 4-amino phenol were mixed in a 25 ml round bottom flask along with 4 ml pyridine as a solvent. This mixture was refluxed for overnight at around 140 °C, cooled and pyridine was evaporated by passing air. Then, the crude product was

purified with 1:1 mixture of dichloromethane and acetone in a column packed with silica gel. This reaction gave 0.15 g (47%) of tan powder. m.p.: 239–241 °C; $^1\text{H NMR}$ (DMSO- d_6) δ : 8.4 (d, $J=7.4$ Hz, 4H), 7.8 (dd, $J=7.4$ Hz, 2H), 7.1 (d, $J=7.1$ Hz, 2H), 6.8 (d, $J=6.9$ Hz, 2H) 9.7 (s, 1H); $^{13}\text{C NMR}$ (DMSO- d_6) δ : 164.3, 157.6, 134.8, 131.9, 130.4, 128.2, 127.7, 127.4, 123.1, 115.9; IR $\nu=1,697, 1,647, 1,588, 1,515, 1,288, 825, 788 \text{ cm}^{-1}$. Anal. Calcd. for $\text{C}_{18}\text{H}_{11}\text{NO}_3$: C, 74.7; H, 3.83. Found: C, 74.51; H, 4.00.

N-(2-aminoimidazolyl)-1,8-naphthalimide (4)

0.13 g (0.81 mmol) of 2-aminoimidazole sulfate was added to 0.02 g (1.01 mmol) 1,8-naphthalic anhydride in a 25 mL round bottom flask along with 4 mL pyridine as solvent. The mixture was refluxed overnight at around 110 °C, cooled and the pyridine evaporated in a fume hood under compressed air. The crude product was washed with acetone and decanted over filter paper. The remaining solid yielded 0.31 g (95%) white powder. m.p. 260 °C; $^1\text{H NMR}$ (DMSO- d_6) δ : 8.55 (dd, $J_{\text{app}} = 6.9$ Hz, 4H), 7.93 (dd, $J_{\text{app}} = 8.3$ Hz, 2H) 6.73–6.67 (m, 3H); $^{13}\text{C NMR}$ (DMSO- d_6) δ : 161.1, 136.1, 135.8, 133.2, 132.9, 132.0, 131.3, 128.2, 127.9, 119.5; IR $\nu=1769, 1735, 1121, 1007, 773 \text{ cm}^{-1}$. Anal. Calcd. for $\text{C}_{18}\text{H}_{11}\text{NO}_3 \cdot 1/2\text{H}_2\text{SO}_4$: C, 59.11; H, 3.28. Found: C, 58.71; H, 3.64.

Photophysical measurements

Fluorescence measurements were done using Jobin-Yvon FluoroMax-3 and UV spectra were recorded using Varian-Cary 50 spectroscopy system. To study the photophysical properties of these three isomers, quantum yields were measured in different solvents like acetonitrile, ethyl ether, ethyl acetate, methanol and hexane. The quantum yield measurements were carried out using Quinine Sulfate dihydrate as standard (quantum yield=0.57) and values are given in "Appendix I" for these three isomeric forms [26]. From the fluorescence spectra, the ortho isomer showed the highest intensities among these three forms in all solvents used. Hence, the trend for quantum yield is observed as Ortho Isomer > Meta Isomer > Para Isomer.

Calculations

The fully optimized geometry of the ground state of the three hydroxy-isomers of *N*-aminophenol 1,8-naphtha-

limdes in the gas phase was calculated by ab initio quantum chemical method at the level of HF/6-31G(d) [27]. The force matrices of the fully optimized structures were found to be positive definite.

Results and discussion

Absorption and fluorescence

For both *ortho* and *meta* isomers, (**1** and **2**) bathochromic shifts in absorption due to solvent polarity were observed as a general trend (spectra and λ_{max} values in supplementary data). In hexanes (a mixture of C_6H_{12} isomers), these compounds displayed similar λ_{max} values at 325 nm and a red-shift in absorbance for the most polar solvent methanol at 335 nm. Interestingly, the *para*-isomer (**3**) displayed a λ_{max} in hexanes at 335 nm which is a higher value than observed for either ethyl acetate, diethyl ether or acetonitrile at $\lambda=327, 329, 331$ nm, respectively. Our explanation for this deviation in solvatochromism is dependent on solvent viscosity. As these compounds have been shown to display rotational dynamics about the *C*-phenyl-*N*-imide bond, **3** is expected to have a lower energy barrier than either *ortho* or *meta* isomers. Because these rotational rates have a dependency on solvent viscosity, i.e. lower rotational frequency at given temperature in higher viscosity solvents, the *para* hydroxy isomer may exhibit paraquinoidal properties that is not possible with the other isomers [28]. Thus hexanes which have a lower viscosity than either acetonitrile or methanol should provide a lower energy barrier to a rotation than other solvents.

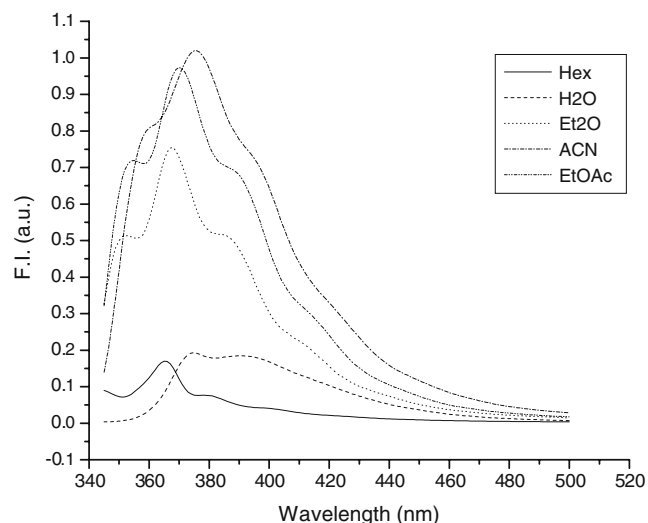


Fig. 2 Fluorescence Spectrum of *ortho* isomer (**1**). [1.0×10^{-5} M] at 25 °C, $\lambda_{\text{exc}}=330$ nm showing SW emission only

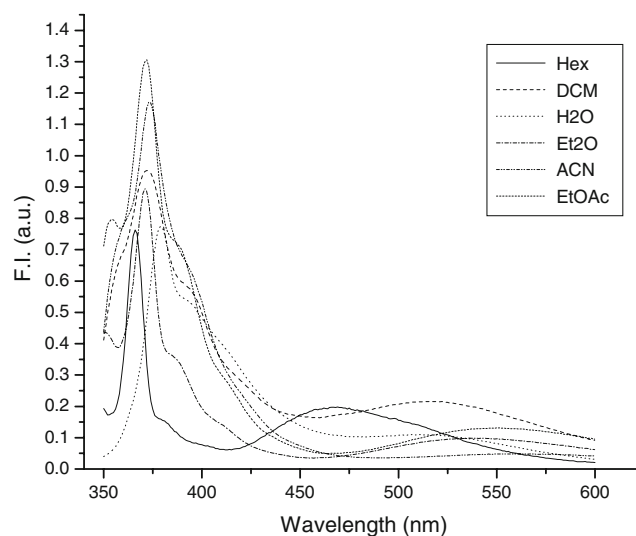


Fig. 3 Fluorescence spectrum of *para* isomer (**3**) mechanism [1.0×10^{-5} M] at 25 °C, $\lambda_{\text{exc}}=335$ nm, showing dual emission via ESEC

Dual fluorescence

For the *ortho* isomer (**1**), dual emission (normal emission and conjugate base emission) via ESIPT mechanism was expected as the hydroxyl group (proton donor) and carbonyl group (proton acceptor) are in fairly close proximity. Upon photoexcitation, there exists the possibility of proton transfer leading to two emissions. As shown in Fig. 2, this isomer displayed only strong SW emission but no tautomer emission.

Along similar lines, trends in fluorescence quantum yields also appear to depend on solvent viscosity. For all three isomers, we observed higher fluorescence quantum yields in methanol and acetonitrile than in hexanes and diethyl ether. While these trends do not correlate in a completely linear relation between viscosity and quantum yield, (i.e. Acetonitrile viscosity=0.345; ethyl acetate 0.426, QY of each at 7.1×10^{-4}), the “loose bolt” effect (i.e. non-radiative decay via internal conversion) appears to apply where higher viscosity solvents hinder non-radiative rotational relaxation of the fluorophore [29].

Conversely, isomer **3** gave two emission bands of various intensities in all solvents used (Fig. 3). This isomer displayed fairly intense dual emission with nonpolar solvent hexanes (366 nm and 466 nm, dielectric constant $\epsilon=2.02$), and less polar solvent dichloromethane (372 nm and 514, $\epsilon=9.08$) and ethyl ether (371 nm and 538 nm, $\epsilon=4.34$), but very weak DF with polar solvents like acetonitrile (375 nm and 550 nm, $\epsilon=36.6$) and water (379 nm and 517 nm, $\epsilon=80$). Next, the 2-aminoimidazole derivative (**4**) was examined for dual fluorescence as the 2-amino proton is positioned to provide a hydrogen bond to imide carbonyl in forming a six-membered ring. In comparison to the phenol derivatives (**1–3**), compound **4** displayed far greater fluorescent quantum yields. However, despite the optimal ring geometry, the fluorescence

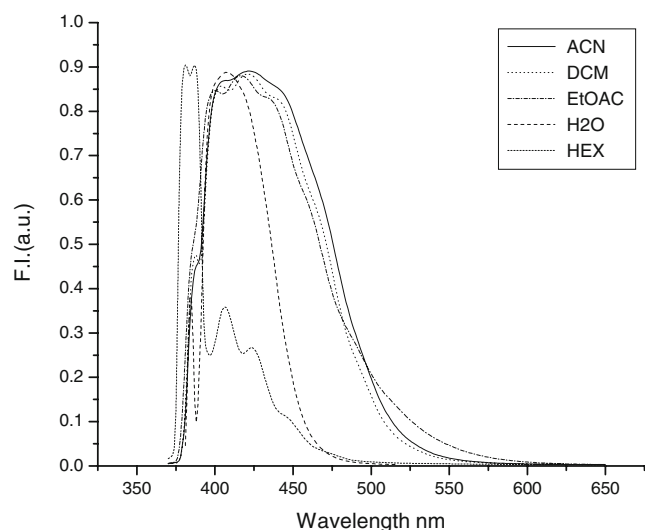


Fig. 4 Fluorescence spectrum of (4). [1.0×10^{-5} M] at 25 °C, $\lambda_{\text{exc}} = 340$ nm showing SW emission

spectra (Fig. 4) show no LW emission, but only SW in the various solvents included with this study.

Quenching effect with DMSO and pyridine

Recent studies have shown that photoexcitation significantly increases the acidity of hydroxy aromatic compounds, [30, 31] and the proton transfer from excited molecule to strong proton acceptor solvents (i.e. hydrogen bonding solvents like DMSO and pyridine) is possible [32, 33]. Hence, to study the effect of strong proton acceptor solvents on the photophysical properties of hydroxysubstituted *N*-aryl 1,8-naphthalimides, these three isomers were titrated with DMSO and pyridine in 0 M–0.035 M range. The fluorescence measurements showed that quenching occurs with these isomers on increasing the concentration of these solvents during titration. In all cases, there was

neither the shift of emission bands nor the appearance of new bands for proton transfer to these solvents, thus indicating the absence of an excited state proton transfer (vide infra for explanation). The fluorescence spectra for these titrations are given in the “Appendix II” section. Graphical analysis of the quenching data is shown in Fig. 5. The Stern-Volmer plot of the steady-state fluorescence intensities in the absence (I_0) and the presence of pyridine (I) shows an upward curvature in the Stern-Volmer plot. Such non-linear curves are observed when the same fluorophore can be quenched by both static and dynamic processes. To obtain an apparent fluorescent quenching constant (K_{app}) which is the product of both static and dynamic quenching constants, (K_S and K_D , respectively), a plot of $[(F_0/F)-1]/[Q]$ gives a linear graph shown in Fig. 6. From the slope of Fig. 5, ortho-isomer **1** shows a large $K_{\text{app}} = 75.5 \text{ mM}^{-2}$ for pyridine and 13.9 mM^{-2} for DMSO, whereas meta-isomer **2** displayed a $K_{\text{app}} = 8.6 \text{ mM}^{-2}$ for pyridine and 18.4 mM^{-2} for DMSO. Para-isomer **3** gave similar K_{app} values in response to fluorescence quenching as the meta-isomer **2** (curve not shown due to similar slope). These K_{app} values represent a marked contrast to previously reported phenol/hydrogen-bonding interactions wherein DMSO shows a much larger quenching constant than with pyridine [34]. Without fluorescent lifetime data we were unable to separate the K_S and K_D terms and therefore report K_{app} as the product of both. However, one explanation for the increased quenching ability of pyridine over DMSO may be due to pi-pi interactions with pyridine. Static quenching is often observed if the fluorophore and quencher can have a stacking interaction [35]. As Fig. 5 indicates, ortho isomer **1** shows a higher K_{app} with pyridine than meta isomer **2**. This difference between isomers is suggestive of a two-point recognition arrangement wherein the phenol proton can interact from a pi-stacked pyridine molecule with much closer proximity than meta isomer **3** (see Fig. 7).

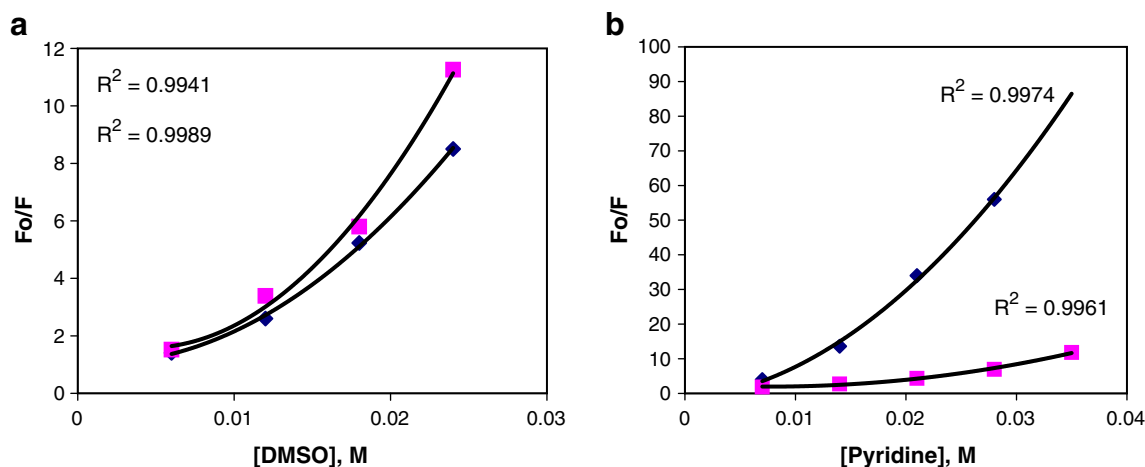


Fig. 5 Quenching of ortho-isomer **1** (full line) and meta isomer **2** (dashed line) in the presence of DMSO (left panel) and pyridine (right panel). F_0 represents fluorescence intensity in the absence of quencher whereas F represents fluorescence intensity with quencher

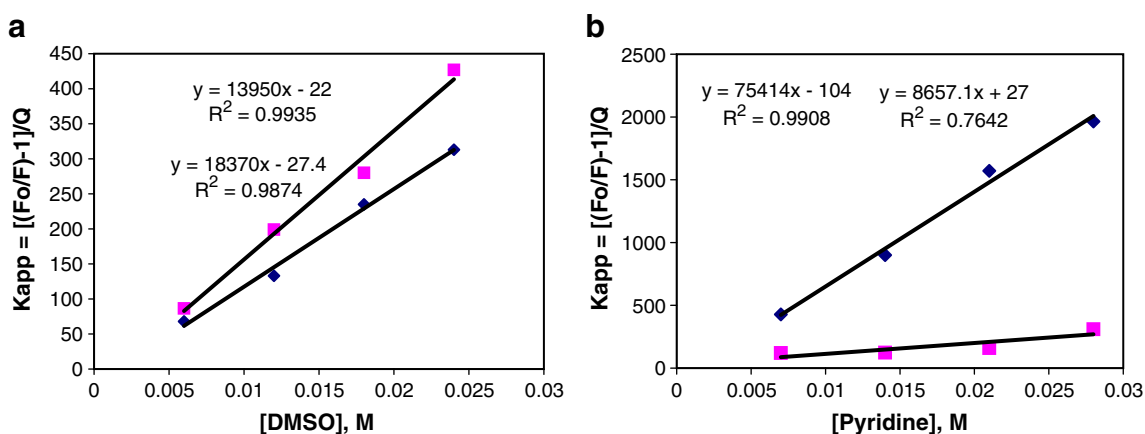


Fig. 6 K_{app} plots of ortho-isomer **1** (full line) and meta isomer **2** (dashed line) in the presence of DMSO (left panel) and pyridine (right panel)

Three-point recognition with an additional sulfonate functionality 1,8-naphthalimides and a phenylboronic acid as the *N*-arene component has been recently reported [36].

Based on the fluorescence spectra obtained from these isomeric dyes, the ortho-isomer (**1**) displayed the highest fluorescence quantum yield relative to the other isomers. According to the ESEC mechanism, conditions which hinder rotation of the *N*-aryl group lead to lower internal conversion rates and higher rates of radiative decay processes. These findings agree with the isomeric properties as well, since an ortho hydroxy phenol provides increased steric hindrance and limits the degree of internal conversion. If an ESIPT photoexcitation process is occurring, a decreased fluorescence intensity should be observed due to quenching of the excited state via internal proton transfer. In addition, a second emission band is indicative of the anionic conjugate base being formed in the excited state. Instead, a second emission band is found only in the spectra for the para isomer. Such dual emission from an electron releasing para-substituted arene, when appended to 1,8-naphthalimides, has been observed via an ESEC photoexcited state mechanism. In the case of para isomer **3**, two rotational conformers exist in the excited state. As pointed out by Bercés et. al, the N-imide:C-aryl dihedral angle influences the short wave (SW) and (LW) emission bands [37]. At dihedral angles close to 90°, SW emission predominates; whereas LW emission can appear when the angle approaches coplanarity at 0°. A coplanar conformation allows extended conjugation and

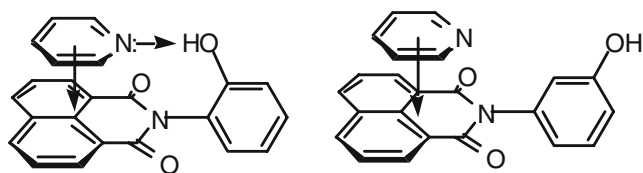


Fig. 7 Proposed binding paradigm for ortho-isomer **1** showing 2-point interaction between naphthalic arene and pyridine as well as hydrogen bonding of hydroxy to pyridine lone pair. The hydrogen bonding interaction is absent in **2**

consequently a longer wavelength. Another useful trend found by comparing the fluorescence wavelengths is seen with the solvent polarity correlation to emission wavelength. In almost all cases, an increase in fluorescence wavelength (red shift) occurs with increased polarity of the solvent. To account for these trends of solvent polarity on fluorescence, an explanation is provided in the next section.

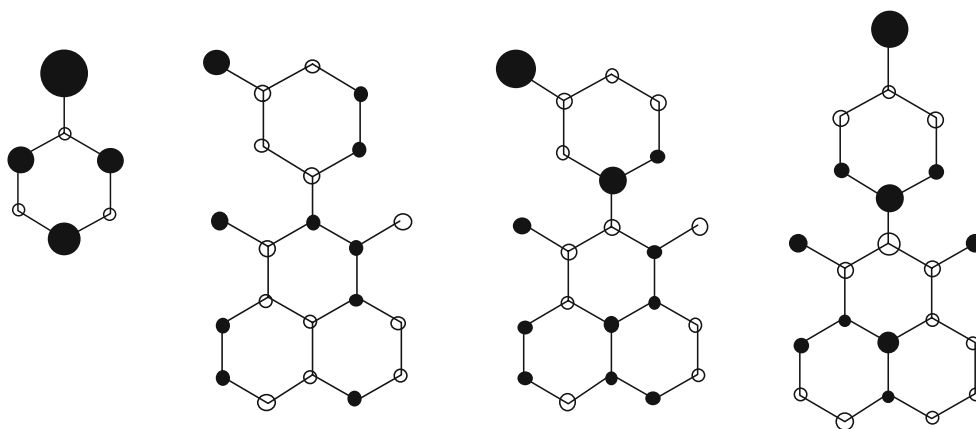
Molecular orbital calculations

Because the conjugate bases of hydroxyarenes like phenols and naphthols can be viewed as derivatives of an odd-alternate hydrocarbon anion, their enhanced acidities are due to the large coefficient on oxygen which is present in the non-bonding molecular orbital (NBMO) [30]. Accordingly, a single electron undergoes photoexcitation from a NBMO to the lowest unoccupied molecular orbital (LUMO), which in the isolated phenol, will not be localized on oxygen. In an uncoupled system, the redistributed charge lowers the basicity of the phenolic oxygen in the excited state, or equivalently, the acidity is enhanced. As a comparative study, quantum chemical calculations were carried out on all three *N*-aminophenol isomers of 1,8-naphthalimides. From our computational results, Fig. 8 provides a graphical depiction of the highest occupied molecular orbitals.

Initial inspection of the molecular orbital coefficients as well as their negative and positive signs (Fig. 7) shows that the para isomer **3** has the higher degree of symmetry with respect to orbital signs and coefficients. Because dipole moments and molecule polarity have been shown to correlate with MO coefficients and sign, para isomer **3** is expected to be the least sensitive to solvent polarity, whereas a greater degree of solvatochromic behavior is expected with isomers **1** and **2**.

Evidence for the occurrence of proton transfer in the excited state is given by a second emission band that represents the conjugate base. Therefore, solvents known for their proton accepting ability (pyridine, DMSO) were added in millimolar

Fig. 8 Molecular orbital representations of pz orbitals for phenol and isomers 1–3 in which NBMO for phenol is evident. MO representations for isomers 1–3 show no alteration in orbital signs and reduced charge density on phenol oxygen



amounts to check for increased proton transfer to solvent relative to the ground state. In the case of the compounds 1–3, addition of either DMSO or pyridine resulted in non-linear fluorescence quenching as evidenced by an upward curving graphs of Fig. 4. Neither the appearance of a new emission band nor a shift of the maximum can be seen in fluorescence spectra. As evidence for ESIPT has been based on the appearance of a second LW band, our data suggest that the phenolic OH group does not form an intramolecular hydrogen bond complex in the excited state. This observation may be due to a phenol system that is strongly coupled to the naphthalimide component. In this case, the π -systems for compounds 1–3 cannot be described as an odd alternate hydrocarbon such as phenol, but rather with both naphthalimide and hydroxyarene as part of the molecular orbital representation. Thus, $S_0 \rightarrow S_1$ photoexcitation does not necessarily occur from the non-bonding molecular orbital (NBMO), as mentioned above at the phenol oxygen atom, but rather from the highest bonding molecular orbital which has less electron density on the oxygen. Molecular orbital coefficients appear to support this conclusion as the coefficients on the phenol oxygen atom were smaller in all cases with the NI dyes than with phenol itself. Geometry optimization for the ortho isomer generated a minimized *N*-imide-*C*-phenol dihedral angle of 82° compared to the other isomer angles around 52° . In this case the pz oxygen orbitals were greatly diminished in electron density and the py orbitals significantly larger. This observation may account for the directional hydrogen bonding between pyridine for isomer 1 relative to meta and para systems [21].

Conclusion

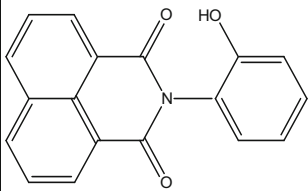
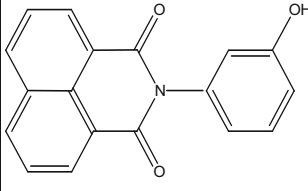
The fluorescence spectral data point to an ESEC mechanism as opposed to a potentially viable mechanism involving ESIPT. This conclusion is based upon three findings from our spectroscopic measurements. Specifically, none of the isomeric phenols displayed their corresponding conjugate base upon

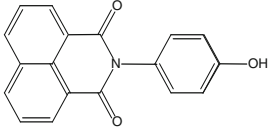
photoexcitation. Rather only isomer 3, which has a para-substituted hydroxyl group, gave a second emission band in the long wavelength region. One reason for the lack of intramolecular proton transfer can be explained by the less than ideal 7-membered ring transition state required for transfer to effectively occur. Fluorescence measurements were conducted with 2-aminoimidazole since the imidazole-NH group has the potential to form a six-membered ring transition state. However, the absence of a second emission band in these experiments also appears to refute the mechanism of an ESIPT process. In addition, fluorescence quantum yield data indicate that the ortho isomer displayed the brightest fluorescence. This result is attributed to less rotational freedom for 1 relative to the other isomers and a decrease in non-radiative decay via internal conversion. If an intramolecular proton transfer from hydroxyl group to imide carbonyl moiety took place, then a decrease in the SW fluorescence band would be expected. Finally, in the presence of hydrogen bonding solvents, no LW emission bands were observed.

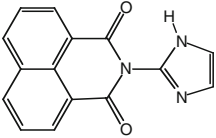
In summary, the data presented suggest that fluorophores based on 1,8-naphthalimides are not so amenable to synthetic designs that may promote proton-transfer for radiative decay pathways such as ESIPT. In this case, *N*-phenyl-1,8-naphthalic imides cannot be synthetically tailored to undergo a LW radiative process that hydroxyflavones typically undergo. Therefore, the inherent electronic properties of the system appear to have a stronger influence than might be anticipated through substitution patterns of proton donor and acceptor groups. In addition, the fluorescence quenching data for isomer 1 show an unexpectedly high K_{app} for pyridine relative to DMSO a solvent that has been shown previously to form stronger hydrogen bonds with phenol. The high K_{app} for pyridine is attributed to a two-point recognition interaction. Plans are currently underway to explore this binding as a fluorescent probe with medicinally relevant pyridine-containing alkaloids such as nicotine, normicotine and anabasine.

Acknowledgements The authors thank the NIH-NIGMS for providing financial support.

Appendix I: photophysical properties

	Absorbance	λ_{ex} (nm)	λ_{em} (nm)	Intensity	Φ_F
Acetonitrile	330(nm), 0.273	330	375	51×10^5	5.2×10^{-3}
Methanol	341(nm), 0.267	330	380	29×10^5	3.1×10^{-3}
Ethyl acetate	330(nm), 0.305	330	370	49×10^5	4.5×10^{-3}
Ethyl Ether	325(nm), 0.270	330	367	38×10^5	3.9×10^{-3}
Hexane	325(nm), 0.234	330	365	8.5×10^5	9.7×10^{-4}
	Absorbance	λ_{ex} (nm)	λ_{em} (nm)	Intensity	Φ_F
Acetonitrile	331.5(nm), 0.293	330	375	50×10^5	4.8×10^{-3}
Methanol	335.50(nm), 0.271	330	390	32×10^5	3.3×10^{-3}
Ethyl acetate	330(nm), 0.267	330	370	41×10^5	4.3×10^{-3}
Ethyl Ether	328.5(nm), 0.283	330	368	29×10^5	2.9×10^{-3}
Hexane	325(nm), 0.166	330	368	8.3×10^5	1.4×10^{-3}

	Absorbance	λ_{ex} (nm)	λ_{em} (nm)	Intensity	Φ_{F}
Acetonitrile	338(nm), 0.221	340	368	7.4×10^5	7.1×10^{-4}
DCM	339(nm), 0.232	340	367	3.3×10^5	3.0×10^{-4}
Ethyl acetate	329(nm), 0.224	340	367	7.4×10^5	7.1×10^{-4}
Ethyl Ether	337(nm), 0.216	340	366	6.4×10^5	6.5×10^{-4}
Hexane	337(nm), 0.472	340	366	5.4×10^5	5.3×10^{-4}

	Absorbance	λ_{ex} (nm)	λ_{em} (nm)	Intensity	Φ_{F}
Acetonitrile	338(nm), 0.223	335	423	18×10^6	1.7×10^{-2}
DCM	342(nm), 0.223	335	421	18×10^6	1.7×10^{-2}
Ethyl acetate	337(nm), 0.222	335	417	18×10^6	1.7×10^{-2}
H ₂ O	341(nm), 0.242	335	434	18×10^6	1.7×10^{-2}
Hexane	337(nm), 0.470	335	407	73×10^5	3.3×10^{-3}

References

- Demchenko A (2005) Lab Chip 5:1210–1223 doi:10.1039/b507447a
- Grabowski Z, Rotkiewicz K, Rettig W (2003) Chem Rev 103:3899–4031 doi:10.1021/cr9407451
- Druzhinin SI, Kovalenko SA, Senyushkina TA, Demeter A, Machinek R, Noltemeyer M, Zachariasse KA (2008) J Phys Chem A 112:8238–8253
- Yoshihara T, Druzhinin SI, Demeter A, Kocher N, Stalke D, Zachariasse KA (2005) J Phys Chem A 109:1497–1509
- Zachariasse KA, Druzhinin SI, Bosch W, Machinek R (2004) J Am Chem Soc 126:1705–1715
- Zachariasse KA, Yoshihara T, Druzhinin SI (2002) J Phys Chem A 106:6325–6333
- Iwashita Y, Sugiyasu K, Ikeda M, Fujita N, Shinkai S (2004) Chem Lett 33:1124–1125 doi:10.1246/cl.2004.1124b
- Haidekker MA, Theodorakis EA (2007) Org Biomol Chem 5:1669–1678 doi:10.1039/b618415dc

9. Kobiros K, Inoue Y (2003) *J Am Chem Soc* 125:421–427 doi:[10.1021/ja028401xd](https://doi.org/10.1021/ja028401xd)
10. Yang CY, Liu Y, Zheng D, Zhu JC, Dai J (2007) *J Photochem Photobiol Chem* 188:51–55 doi:[10.1016/j.jphotochem.2006.11.017e](https://doi.org/10.1016/j.jphotochem.2006.11.017e)
11. Jones G, Jimenez JAC (2001) *J Photochem Photobiol B-Biology* 65:5–12
12. Papper V, Kharlanov V, Schadel S, Maretzki D, Rettig W (2003) *Photochem Photobiol Sci* 2:1272–1286
13. Yang J-S, Hwang C-Y, Chen M-Y (2007) *Tet Lett* 48:3097–3102
14. Klymchenko AS, Demchenko AP (2002) *J Am Chem Soc* 124:12372–12379 doi:[10.1021/ja0276691b](https://doi.org/10.1021/ja0276691b)
15. Klymchenko AS, Ozturk T, Pivovarenko VG, Demchenko APN (2003) *J Chem* 27:1336–1343 doi:[10.1039/b302965d](https://doi.org/10.1039/b302965d)
16. Weller AH (1956) *Z Electrochem* 60:1144
17. McMorro D, Kasha M (1984) *J Phys Chem* 88:2235–2243 doi:[10.1021/j150655a012](https://doi.org/10.1021/j150655a012)
18. Formosinho SJ, Arnaut LG (1993) *Photochem Photobiol A-Chemistry* 75:21–48
19. Legourrierec D, Ormson SM, Brown RG (1994) *Prog React Kin* 19:211–275
20. Santara S, Krishnamoorthy G, Dogra SK (2000) *J Phys Chem A* 104:476–482 doi:[10.1021/jp992678a](https://doi.org/10.1021/jp992678a)
21. Yushchenko DA, Bilokin MD, Pyvovarenko OV, Duportail G, Mely Y, Pivovarenko VG (2006) *Tet Lett* 47:905–908 doi:[10.1016/j.tetlet.2005.11.160](https://doi.org/10.1016/j.tetlet.2005.11.160)
22. Inoue Y, Jiang P, Tsukada E et al (2002) *J Am Chem Soc* 124:6942–6949 doi:[10.1021/ja0168581](https://doi.org/10.1021/ja0168581)
23. Demeter A, Bércés T, Hinderberger J, Timári G (2003) *Photochem Photobiol Sci* 2:273–281 doi:[10.1039/b210592f](https://doi.org/10.1039/b210592f)
24. Demeter A, Bércés T, Biczok L, Wintgens V, Valat P, Kossanyi J (1996) *J Phys Chem* 100:2001–2011 doi:[10.1021/jp951133n](https://doi.org/10.1021/jp951133n)
25. Cao H, Chang V, Hernandez R, Heagy MD (2005) *J Org Chem* 70:4929–4934 doi:[10.1021/jo050157f](https://doi.org/10.1021/jo050157f)
26. Gillespie AM (1985) *A manual of fluorometric and spectrophotometric experiments*. Gordon and Breach Science, New York
27. Gaussian 03, Revision D.01, Frisch MJ, Trucks GW, Pople JA et al (2004) Gaussian, Inc., Wallingford CT
28. Hoa GHB, Kossanyi J, Demeter A, Biczok L, Bércés T (2004) *Photochem Photobiol Sci* 3:473–482 doi:[10.1039/b313804f](https://doi.org/10.1039/b313804f)
29. Anslyn EV, Dougherty DA (2006) *Modern physical organic chemistry*. University Science Books, Sausalito, CA, p 953
30. Tolbert LM, Haubrich JE (1994) *J Am Chem Soc* 116:10593–10600 doi:[10.1021/ja00102a028b](https://doi.org/10.1021/ja00102a028b)
31. Weller A (1961) *Progress in Reaction Kinetics* vol. 1. In: Porter G (ed) Pergamon, p.187–214
32. Herbich J, Rettig W, Thummel RP, Waluk J (1992) *Chem Phys Lett* 195:556–562 doi:[10.1016/0009-2614\(92\)85562-O](https://doi.org/10.1016/0009-2614(92)85562-O)
33. Biczok L, Valat P, Wintgens V (1999) *Phys Chem Chem Phys* 1:4759–4766 doi:[10.1039/a904520a](https://doi.org/10.1039/a904520a)
34. Joesten MD, Schaad L (1974) *Hydrogen bonding*. J Marcel Dekker, Inc, New York
35. Lakowicz JR (1999) *Principles of Fluorescence Spectroscopy*, 2nd ed. Kluwer Academic/Plenum, p 243
36. Coskun A, Akkaya EU (2004) *Org Lett* 6:241–243 doi:[10.1021/ol0488744](https://doi.org/10.1021/ol0488744)
37. Wintgens V, Valat P, Kossanyi J, Demeter A, Biczok L, Bércés TN (1996) *New J Chem* 20:1149–1158